INTERNATIONAL JOURNAL OF AGRICULTURE & BIOLOGY
ISSN Print: 1560–8530; ISSN Online: 1814–9596
18F–096/2018/20–10–2363–2370
DOI: 10.17957/IJAB/15.0823
http://www.fspublishers.org

Full Length Article

Proteomic Analysis of the Secretory Proteins from *Phytophthora infestans* under Nitrogen Deficiency using Label-free LC-MS

Ping Yu[†], Chao Dong[†], Chunxin Yao, Yumei Ding and Xiaogang Zhou[*]
Key Laboratory of Southwestern Crop Gene Resources and Germplasm Innovation, Ministry of Agriculture and Yunnan Provincial Key Laboratory of Agricultural Biotechnology, Biotechnology and Germplasm Resources Institute, Yunnan Academy of Agricultural Sciences, Kunming 650205, China
[*]For correspondence: 1124746288@qq.com
[†]These authors contributed equally to this study

Abstract

Phytophthora infestans causes the late blight disease in potato, and its effectors have a potential role in its pathogenicity. Nitrogen is a key nutrient source affecting the growth and development of microbiota. Differentially expressed proteins secreted by the *P. infestans* strain NOD-1 were analyzed using label-free liquid chromatography–mass spectrometry quantitative proteomics in a complete medium or under nitrogen-deficient conditions to understand whether nitrogen stress promoted the secretion of more pathogenic proteins by *P. infestans.* A total of 5615 unique peptides and 1188 proteins were identified. Moreover, 93 differentially expressed proteins (containing signal peptides of Crinkling and necrosis-inducing protein and Arginine-X-leucine-arginine) and 28 specific proteins (localized extracellularly, in the cytoplasm, and in the plasma membrane) were detected under nitrogen-deficient conditions. Furthermore, 27 important effectors (mainly apoplastic and cytoplasmic), which had a potential role in the infection process, were screened. This study showed that the pathogenicity of *P. infestans* was enhanced under nitrogen-deficient conditions through the expression of effectors, particularly the cytoplasmic effectors.

Keywords: Effectors; *Phytophthora infestans*; Proteomics; Secretory proteins

Introduction

Phytophthora infestans causes the late blight disease in potato, which is considered the most harmful crop disease worldwide leading to a substantial reduction in potato production and causing a loss of more than $12 billion (Sanju *et al.*, 2015). In the infection process, *P. infestans* secretes a diverse range of effectors that interfere with the host's defense response and promote colonization by *P. infestans* (Göhre and Robatzek, 2008; Vetukuri *et al.*, 2017). Effectors are divided into two groups on the basis of the target site in plant cells: apoplastic and cytoplasmic. The apoplastic effectors are secreted into the plant extracellular space. They interact with extracellular inhibitors [response factors, such as glucanase inhibitor proteins (GIP1 and GIP2); extracellular serine protease inhibitors (EPI1 and EPI10); and extracellular cysteine protease inhibitors (EPIC1 and EPIC2]. The cytoplasmic effectors enter the host cytoplasm and interact with the target within the host cell, for example Arginine-X-leucine-arginine (RxLR) class effectors containing the RxLR motif and Crinkling and necrosis-inducing protein (CRN) effectors containing the Leucine-phenylalanine-leucine-alanine-lysinemotif (Dong *et al.*, 2015; Vetukuri *et al.*, 2017). Previous studies have identified about 563 RxLR effectors and 196 CRN effectors through genomic sequence analysis and prediction (Haas *et al.*, 2009).

Several fungal genes were induced under nitrogen-limiting conditions (Snoeijers *et al.*, 2000). Nitrogen regulation was important in pathogenicity. A large number of studies focused on nitrogen regulation in *Magnaporthe oryzae*. Nitrogen starvation could induce *M. oryzae* to secrete pathogenic proteins (Donofrio *et al.*, 2009; Wang *et al.*, 2011). However, no study was conducted on nitrogen regulation in *P. infestans.*

This study used label-free quantitative proteomic approaches to explore whether nitrogen affected the pathogenicity of *P. infestans* through the expression of effectors.

Materials and Methods

Strain Culture and Preparation of Secretory Proteins

P. infestans NOD-1 was transferred from a test tube to a solid culture medium (rye 70.0 g/L, tomato juice 150 mL/L, agar powder 8.0 g/L, amoxicillin 100 mg/L, pentachlorobenzene 30 mg/L, rifampicin 10 mg/L and

To cite this paper: Yu, P., C. Dong, C. Yao, Y. Ding and X. Zhou, 2018. Proteomic analysis of the secretory proteins from *Phytophthora infestans* under nitrogen deficiency using label-free LC-MS. *Int. J. Agric. Biol.*, 20: 2363–2370

natamycin 10 mg/L) and incubated at 17°C for 7 days in the incubator. The nitrogen deficiency was treated using the methods proposed by Zhou *et al.* (2016). A nitrogen-deficient culture medium (0.52 g KCl, 0.52 g $Mg_2SO_4 \cdot 7H_2O$, 1.52 g KH_2PO_4, 10 g glucose, and 2 mL of trace elements in 1.0 L of H_2O) was used for this purpose. The incubation temperature was changed from 17°C to 28°C. Finally, the filtrate was collected. The filtrates from two parts of mycelia were placed on ice, and 100% $(NH_4)_2SO_4$ was slowly added to the filtrates with stirring at 4°C overnight to precipitate proteins, followed by centrifugation at 4°C and 10,000 rpm for 10 min. The precipitate was dissolved in deionized water, transferred to a dialysis bag with a cut off range of 1 kDa, and placed in deionized water at 4°C. The dialysate was replaced every 4 h. The dialyzed proteins were freeze-dried and reserved.

Protein Cleavage and Quantification

The samples were added in 300 μL of lysis buffer, sonicated, boiled for 15 min, and centrifuged at 12,000 rpm for 30 min. The supernatants were collected, and the protein concentration was determined with a Bicinchoninic Acid Protein Assay Kit (Bio-Rad, USA).

Protein Digestion

The samples were treated with Zeba (100 μL each), and dithiothreitol was added to the samples at a final concentration of 100 m*M*. Subsequently, the samples were boiled for 5 min, cooled down to 20°C, and mixed with 200 μL of UA buffer (8 *M* urea, 150 m*M* Tris-HCl, pH 8.0). The mixture was then transferred into a 30-kDa ultracentrifugation tube and centrifuged at 14,000 g for 15 min. Another 200 μL of UA buffer was added to the tube, followed by centrifugation at 14,000 g for 15 min. The filtrate was discarded. Then, 100 μL of iodoacetamide was added, vibrated at 600 rpm for 1 min, and then centrifuged at 14,000 g for 10 min at 20°C for 30 min in the dark. Further, 100 μL of UA buffer was added and centrifuged at 14,000 g for 10 min twice. Thereafter, 100 μL of NH_4HCO_3 buffer was added to the precipitate, followed by centrifugation at 14,000*g* (Space is needed between digit and all units except ºC and %) for 10 min twice. The protein suspension was digested with 40 μL of trypsin. The samples were oscillated at 600 rpm for 1 min and then incubated at 37°C for 18 h. The collection tube was replaced, the samples were centrifuged at 14,000 g for 10 min, and then the filtrate was collected. The filtrate was desalted using a C18-SD Extraction Disk Cartridge, and its concentration was evaluated at and optical density of 280 nm.

Liquid Chromatography–mass spectrometry Analysis

The separation was carried out using EASY-nLC1000. Solution A was 0.1% formic acid–acetonitrile aqueous solution (2% acetonitrile). Solution B was 0.1% formic acid–acetonitrile aqueous solution (84% acetonitrile). Briefly, 5 μL of peptides were separated on a pre-equilibrated RP-C18 column (Thermo EASY column, 0.15 ×100 mM^2) with a gradient program as follows: 0–45% B (100 min), 45–100% B (8 min), and 100% B (12 min). The flow rate was set at 400 nL/min. The hydrolysate was separated using capillary high-performance liquid chromatography and analyzed using mass spectrometry (MS) with a Q-Exactive mass spectrometer (Thermo Finnigan) with an analysis time of 120 min, a positive ion detection method, and a precursor ion scanning range of 300–1800 *m*/*z*. Survey scans were acquired at a resolution of 70,000 at 200 *m*/*z*, and the resolution for the HCD (higher-energy collisional dissociation) spectra was set to 17,500 at 200 *m*/*z*. The MS data were analyzed and searched using the MaxQuant software (version 1.3.0.5) and the uniprot_ phytophthorainfestans_18465_20151221.fasta, respectively.

Bioinformatics Analysis

Signal P 4.1 was used to predict the signal peptide of target proteins. WoLF PSORT (http://www.genscript.com/wolf-psort) was used to predict the subcellular localizations of target proteins. TMHMM 2.0 (http://www.cbs.dtu.dk/services/TMHMM/) was used to predict the numbers of transmembrane helices in proteins, and this program was rated the best to rigorously discriminate transmembrane helix (TMH) from others (Bigelow and Rost, 2009). The functional annotation of differentially expressed proteins under nitrogen-deficient and complete culture conditions was performed using the Gene Ontology (GO) and Web Gene Ontology Annotation (WEGO) plot (http://wego.genomics.org.cn/cgi-bin/wego/). The Kyoto Encyclopedia of Genes and Genomes (KEGG) (http://www.kegg.jp/ke gg/) was used to predict the metabolic pathways of proteins. Self-optimized prediction method with alignment (SOPMA) (https://npsa-prabi.ibcp.fr/cgi-bin/npsa_automat.pl?page=npsa_sopma. html) was used to predict the secondary structure of proteins. Multiple Em for motif elicitation (MEME) (http://meme-suite.org/) and simple modular architecture research tool (SMART) (http://smart.embl-heidelberg.de/) were employed to predict the conserved motif and conserved domain, respectively.

Results

Identification of Differentially Expressed Proteins

The differences in secretory proteins from *P. infestans* were compared under nitrogen-deficient and complete culture conditions using the high-throughput label-free proteome method to understand the effect of nitrogen deficiency on the pathogenicity of *P. infestans*. A total of 5615 unique peptides and 1188 proteins were identified. The Intensity-based absolute quantification (iBAQ) values of proteins were used to characterize the protein abundance.

A total of 655 proteins were secreted by *P. infestans* under nitrogen-deficient and complete culture conditions. Moreover, 225 and 9 proteins were present exclusively under nitrogen-deficient and complete culture conditions, respectively. A total of 399 proteins were differentially expressed with a *P* value $\leqslant 0.01$ and a fold change of $\geqslant 2$ at the protein level. Six of these proteins belonged to the CRN family, and one protein was the RxLR effector. Signal peptide prediction of 399 proteins showed that 87 proteins contained signal peptides (Table 1). Three proteins among the 234 specific proteins belonged to the CRN family. Signal peptide prediction showed that 25 proteins contained signal peptides (Table 2).

Bioinformatics Analysis

A total of 93 differentially expressed proteins containing signal peptides of CRN and RxLR were mapped and domain analyzed. The results showed that 76.6% of the proteins were localized extracellularly, 8.5% were in the mitochondrial inner membrane, 9.6% were in the cytoplasm, 2.1% were in the endoplasmic reticulum, and 3.2% were in the plasma membrane. Of the 93 differentially expressed proteins, 14 proteins contained domains. Of the 28 specific proteins, 85.7% were localized extracellularly, 10.7% were in the cytoplasm, and 3.6% were in the plasma membrane. A total of 68 of the 93 proteins were involved in metabolic activities, response to a stimulus, and cellular processes (Fig. 1).

The KEGG analysis showed that the most differentially expressed proteins were not involved in the metabolic pathway. Moreover, a few proteins were involved in protein export, pentose and glucuronate interconversion, cyanoamino acid metabolism, starch and sucrose metabolism, folate biosynthesis, N-glycan biosynthesis, phagosome activity, thiamine metabolism, and riboflavin metabolism (Fig. 2).

For screening, the secondary structure, conserved motifs, and conserved domains of 27 effectors were analyzed using SOPMA, MEME, and SMART, respectively. The data showed that these effectors were composed mainly of alpha helix, beta turn, and random coil, and the proportion of alpha helix was significantly higher than that of the beta-turn. The Q646V6 protein did not have the beta-turn (Fig. 3).

The conservative motif analysis of 27 effectors revealed that only 6 CRN effectors contained conserved motifs. Four of these six proteins contained three conserved motifs at consistent positions. The other two proteins contained only one conserved motif, and the position of this motif was also slightly different (Fig. 4).

The SMART online software analysis showed that 16 proteins contained conserved domains (Fig. 5). Interestingly, PexRD2 family–secreted RxLR effector peptide and CRN-like proteins did not contain conserved domains.

Discussion

The apoplastic effectors included enzyme inhibitor family, small cysteine-rich proteins, and neuropeptide-like protein family. Enzyme inhibitors generally inhibit host plant protease activity. *Phytophthora* glucanase inhibitory proteins (GIPs) are capable of inhibiting the activity of oligosaccharides and endoglucanases (Rose *et al.,* 2002; Martins *et al.,* 2014). GIP is thought to be a defense-capable molecule that inhibits the degradation of beta-1,3/1,6-glucan in plant cell walls. The cysteine protease inhibitors, EPIC1 and EPIC2, are a class of protease inhibitors secreted by *P. infestans* (Tian *et al.,* 2007). EPI1 and EPI10 are serine protease inhibitors having a defensive function in the interaction with the plants (Tian and Kamoun, 2005). In the present study, the expression of GIPs, protease inhibitor, and cystatin-like cysteine protease inhibitor were three to five times higher than that in control sunder nitrogen-deficient conditions. This suggested that nitrogen was environmentally important for the infectivity of *P. infestans*. As a family of extracellular proteins, elicitins can induce allergic necrosis and other resistance-related physiological and biochemical changes in tobacco. The expression of elicitins INF4 (derived from *P. infestans*) and INF5 was 4.96 and 2.21 times higher than that in controls, respectively. However, these INF proteins may be surface- or cell wall–associated glycoproteins. They can interact with plant cells during infection (Sanju *et al.,* 2015).

The data showed that cytoplasmic effectors, including RxLR and CRN effectors, were upregulated under nitrogen-deficient conditions. Cytoplasmic effectors interfere with immunity the plant cells. They are important in virulence functions of effectors (Damme *et al.,* 2012; McLellan *et al.,* 2013). For example, SNE1 and CRN8 from *P. infestans* can modify host cell physiology (Damme *et al.,* 2012). The RxLR effectors from oomycetes have a variety of functions such as inhibiting B cell lymphoma-2-associated X protein–induced cell death, suppressing pathogen-associated molecular pattern (PAMP)-triggered immunity and effector-triggered immunity functions, inducing cell death, and controlling plant defense response (Hiss *et al.,* 2008). RxLR effectors may be localized to various compartments of the plant cell, such as nucleus, cytoplasm, plasma membrane, and so on (Caillaud *et al.,* 2012). They can suppress host plant RNA-silencing mechanisms (Vetukuri *et al.,* 2017). The present study showed that the expression of a PexRD2 family–secreted RxLR effector peptide was upregulated more than 4.8 times under nitrogen-deficient conditions. Mitogen-activated protein kinase (MAPK) cascades are vital in plant immune signaling pathways, transducing the perception of invading pathogens into effective defense responses (King *et al.,* 2014). MAPKs are phosphorylated on these residues by MAPK kinases (MAPKKs); in turn, these MAPKKs are regulated through phosphorylation by MAPKK kinases (MAPKKKs) (Chang and Karin, 2001).

Table 1: Identification of differentially expressed proteins induced by nitrogen deficiency in *Phytophthora infestans*using label-free LC-MS

Protein IDs	Description	SC [%]	iBAQ C	iBAQ N	N/C	*P* value	SP	TMHs	Subcellular localization
D0NNF1	Crinkler (CRN) family protein	40.8	2152133	14357000	6.67	1.64E-06	N	0	Cytoplasmic
D0N3X0	Putative uncharacterized protein	22.4	3937600	41227000	10.47	1.68E-06	Y	0	Extracellular
D0MZ63	Cysteine protease family C01A	28.6	19060000	125993333	6.61	5.52E-06	Y	0	Extracellular
D0P2Q4	Ribosomal protein	45	67103333	406220000	6.05	6.08E-06	Y	0	Extracellular
D0MXI8	Berberine-like protein	43.2	8801467	51883667	5.89	1.35E-05	Y	1	Extracellular
D0P3I9	Protein disulfide-isomerase	47.3	28247333	168290000	5.96	2.18E-05	Y	0	Cytoplasmic
D0N7W0	GamMa-glutamyl hydrolase	31.9	2165807	23806667	10.99	2.33E-05	Y	0	Extracellular
D0NNQ8	1,3-beta-glucanosyltransferase	45.4	71584000	313280000	4.38	3.11E-05	Y	0	Extracellular
D0NCU6	Small cysteine rich protein SCR108	18.3	3110400	26836333	8.63	3.41E-05	Y	0	Extracellular
D0MUK6	Purple acid phosphatase	33.9	67153667	413703333	6.16	4.82E-05	Y	0	Extracellular
D0MXT1	Endo-1,3(4)-beta-glucanase 1	10.9	1321900	3538033	2.68	5.59E-05	Y	0	Extracellular
D0N7M0	Putative uncharacterized protein	13.9	4174733	42256667	10.12	6.02E-05	Y	0	Extracellular
D0NNB0	Putative uncharacterized protein	19.8	13311067	85416667	6.42	6.90E-05	Y	0	Extracellular
D0NUT6	Crinkler (CRN) family protein	43.4	3049433	82706667	27.12	9.33E-05	N	0	Cytoplasmic
D0NDK0	Endoglucanase	25	2180733	37684000	17.28	9.38E-05	Y	0	Extracellular
D0MZR2	Putative uncharacterized protein	22.4	1071305	8693233	8.11	9.96E-05	Y	0	Extracellular
D0NHS4	Cysteine protease family C01A	37	11252933	67932667	6.04	0.0001	Y	0	Extracellular
D0P2B8	Putative uncharacterized protein	27.8	8845500	65801333	7.44	0.0001	Y	0	Extracellular
D0NHQ0	Glycoside hydrolase	20.8	17592333	74096667	4.21	0.0001	Y	1	Extracellular
D0NR25	Calreticulin	62.3	25222667	137783333	5.46	0.0001	Y	0	Extracellular
D0NL42	Glycine-rich protein	28.7	18906333	126616667	6.70	0.0001	Y	0	Extracellular
D0NIL2	PexRD2 family secreted RxLR effector peptide	18.2	9009533	43306000	4.81	0.0001	Y	0	Extracellular
D0N2B4	Putative uncharacterized protein	34.8	223743333	1122966667	5.02	0.0002	Y	0	Extracellular
D0NVM5	Carbohydrate esterase	14.1	5483400	38322667	6.99	0.0002	Y	0	Extracellular
D0NUA4	NPP1-like protein	54.2	157986667	941083333	5.96	0.0002	Y	0	Extracellular
A1L017	Cystatin-like cysteine protease inhibitor EPC2B	67.2	95413667	258850000	2.71	0.0002	Y	0	Extracellular
D0MVR3	Putative uncharacterized protein	18.8	5528000	51244667	9.27	0.0002	Y	0	Extracellular
D0NUR9	Crinkler (CRN) family protein	41.5	736290	25714000	34.92	0.0002	N	0	Cytoplasmic
D0MS99	Pectinesterase	19.5	1089193	11255667	10.33	0.0002	Y	0	Extracellular
A0A0F7KIH7	Effector protein Avr3a_EM (Fragment)	44.2	7303867	80934333	11.08	0.0003	Y	0	MIM
D0NDH2	Putative uncharacterized protein	21.5	1092065	6788867	6.22	0.0003	Y	0	MIM
D0MQ88	Glucan 1,3-beta-glucosidase	50.3	196780000	655616667	3.33	0.0003	Y	0	Extracellular
Q8H6Z6	Crinkling and necrosis-inducing protein CRN1	40.4	479643	5202267	10.85	0.0003	N	0	Cytoplasmic
D0NLW3	Protein kinase	2.9	352410	3115333	8.84	0.0004	Y	1	Extracellular
D0NYL7	Putative uncharacterized protein	42.8	6226567	61557333	9.89	0.0004	Y	0	Extracellular
D0N6P9	Peptidase, putative	23.2	1040357	12319667	11.84	0.0004	Y	1	Extracellular
D0MWL3	Pectinesterase	41.1	1819280	39029667	21.45	0.0004	Y	0	Extracellular
D0N0L9	Glycosyl transferase, putative	26.5	132350000	524790000	3.97	0.0005	Y	0	Extracellular
Q8S315	Putative exo-1,3-beta-glucanase	21.3	1034127	31160000	30.13	0.0005	Y	1	Extracellular
D0MVC6	Protease inhibitor Epi2	53.3	39223333	186593333	4.76	0.0005	Y	0	Extracellular
D0NNS5	Polysaccharide lyase	7.2	608670	4920100	8.08	0.0005	Y	0	Extracellular
D0NWW5	Putative uncharacterized protein	9.1	4870967	25042000	5.14	0.0006	Y	0	Extracellular
D0MSJ4	Putative uncharacterized protein	21.3	36555000	179786667	4.92	0.0007	Y	0	Extracellular
D0MT51	Glycoside hydrolase	13.4	1790647	23508333	13.13	0.0009	Y	1	Plasma membrane
D0N3D4	Putative GPI-anchored serine-rich tenascin-like glycoprotein	30.1	4482533	14214000	3.17	0.0010	Y	0	Extracellular
D0NY56	Alkaline phosphatase	33.7	3454167	20223000	5.85	0.0010	Y	0	MIM
D0MY50	Cellulose-binding elicitor lectin (CBEL)	8.2	2439700	9433800	3.87	0.0011	Y	0	Extracellular
D0MUS3	Putative uncharacterized protein	23.1	23816333	122013333	5.12	0.0012	Y	1	Extracellular
D0NID9	Neutral alpha-glucosidase	3	73636.5	1018250	13.83	0.0013	Y	0	Extracellular
D0NIG7	Putative uncharacterized protein	2.7	9344133	26334667	2.82	0.0014	Y	0	Extracellular
A1L019	Cystatin-like cysteine protease inhibitor EPIC4	19.2	26435667	110096667	4.16	0.0015	Y	0	Extracellular
D0N8P1	Putative uncharacterized protein	27.1	28272333	125023333	4.42	0.0016	Y	0	Extracellular
Q646V6	Phytotoxin-like SCR74	59.5	5305900	77026333	14.52	0.0017	Y	0	Extracellular
D0NFV4	Thioredoxin-like protein	41.2	3435600	20177000	5.87	0.0017	Y	0	Cytoplasmic
D0N885	Crinkler (CRN) family protein	10.4	486920	7917667	16.26	0.0017	N	1	Cytoplasmic
Q940X1	Endopolygalacturonase	16.3	94848667	365833333	3.86	0.0018	Y	0	Extracellular
D0P3R6	Elicitin-like protein INF4	52.5	32636333	161826667	4.96	0.0018	Y	1	Extracellular
D0P3W0	Putative uncharacterized protein	15.5	19903000	51260333	2.58	0.0020	Y	0	Extracellular
D0MXT2	Endo-1,3(4)-beta-glucanase	16.2	935787	4834633	5.17	0.0023	Y	0	Extracellular
D0MRY5	Carbohydrate-binding protein	2.3	1478550	25338333	17.14	0.0023	Y	1	Extracellular
D0N2Y9	Heat shock protein 90	5.6	129660	1348067	10.40	0.0024	Y	0	Endoplasmic reticulum lumen
D0NXV5	Glutathione peroxidase	25.4	18620667	55933333	3.00	0.0025	Y	0	Plasma membrane
Q2M440	Cutinase	18.7	2669950	56643667	21.22	0.0026	Y	0	Extracellular
D0NER9	Metalloprotease family M13	9.9	1572337	7523600	4.78	0.0026	Y	0	Extracellular
B1AC88	Glucanase inhibitor protein 3	19.8	5631667	28965333	5.14	0.0026	Y	0	Extracellular
D0NCR4	Mucin-like protein	2.6	400955	5371067	13.40	0.0027	Y	1	Extracellular
D0MZG4	Glycoside hydrolase	9.7	616210	4053367	6.58	0.0027	Y	0	Extracellular
D0NUJ8	Putative uncharacterized protein	11	7334867	35371000	4.82	0.0027	Y	0	Extracellular
D0NSN5	Ribonuclease	23.6	507196667	1595733333	3.15	0.0028	Y	0	Extracellular
D0NXB9	Chitinase	50	575300000	2173133333	3.78	0.0029	Y	0	Extracellular
D0MW00	Peptidyl-prolyl cis-trans isomerase	23.9	1134745	15626000	13.77	0.0029	Y	0	MIM
D0N8P5	Predicted GPI-anchored protein	33.3	1605450	10218167	6.36	0.0030	Y	0	Extracellular
D0NGW7	PpiC-type peptidyl-prolyl cis-trans isomerase	64.2	17126000	116760000	6.82	0.0032	Y	0	MIM
Q8S316	Putative endo-1,3-beta-glucanase	53.1	34758000	120148667	3.46	0.0032	Y	0	Extracellular

Table 1: Continued

Table 1: Continued

D0NIC0	Putative uncharacterized protein	17.5	12707000	34813000	2.74	0.0033	Y	0	Extracellular
D0N4L1	Putative uncharacterized protein	17.3	4728867	17107333	3.62	0.0033	Y	0	Extracellular
D0MVC9	Protease inhibitor Epi1	28.2	11780367	39842000	3.38	0.0034	Y	0	MIM
D0N5D5	Putative uncharacterized protein	4.9	7723967	36809000	4.77	0.0037	Y	1	Extracellular
D0MY26	Putative uncharacterized protein	6.6	25006533	113497667	4.54	0.0039	Y	0	Extracellular
D0MR13	Luminal-binding protein 3	32.5	14366033	76774667	5.34	0.0043	Y	0	Endoplasmic reticulum lumen
D0NP00	GPI-anchored leucine-rich lipoprotein	7.4	1534177	9527500	6.21	0.0046	Y	0	Extracellular
D0N631	Putative uncharacterized protein	35	2714867	6074800	2.24	0.0047	Y	0	Cytoplasmic
D0N630	Putative uncharacterized protein	15.1	957810	3314100	3.46	0.0053	Y	0	Extracellular
Q9AT27	Beta-glucosidase/Xylosidase	20.6	64040333	191226667	2.99	0.0055	Y	0	Extracellular
Q944V9	Elicitin-like INF5	17.9	732970000	1622900000	2.21	0.0059	Y	0	Extracellular
Q2M402	CRN-like CRN11	21.6	932783	21584000	23.14	0.0059	N	0	Cytoplasmic
P02768-1	ALB Isoform 1 of Serum albumin precursor	25.3	1049335	16938000	16.14	0.0064	Y	0	MIM
D0NSG4	SCP-like extracellular protein	5.2	2519033	8013967	3.18	0.0066	Y	1	Extracellular
D0NGW0	Putative uncharacterized protein	7.3	698133	3154433	4.52	0.0073	Y	0	Extracellular
D0NQ14	Putative uncharacterized protein	11	78993667	180813333	2.29	0.0076	Y	0	Extracellular
D0N359	Catalase-peroxidase, putative	22	6837300	39953667	5.84	0.0076	Y	0	Extracellular
D0NF93	SCP-like extracellular protein	10	1858837	11149733	6.00	0.0078	Y	0	Extracellular
D0NMH3	Glucanase inhibitor protein	2.7	8196200	31690000	3.87	0.0080	Y	0	Extracellular

MIM, Mitochondrial inner membrane; SC, sequence coverage; SP, signal peptide

Table 2: Identification of specifically expressed proteins induced by nitrogen deficiency in *Phytophthora infestans* using label-free LC-MS

Protein IDs	Description	SC [%]	iBAQ C	iBAQ N	SP	TMHs	Subcellular localization
A2CLL0	Suppressor of necrosis 1	6.9	–	17266500	Y	0	Extracellular
D0MS69	Putative uncharacterized protein	3	–	884657	Y	0	Extracellular
D0MT81	Serine protease family S33, putative	4.3	–	402600	Y	0	Extracellular
D0MTB4	Lactase-phlorizin hydrolase, putative	11.5	–	7132100	Y	1	Plasma membrane
D0MWY9	Calcineurin-like phosphoesterase	7.6	–	599330	Y	0	Extracellular
D0N1J0	Protein kinase	2.5	–	619330	Y	1	Extracellular
D0N3Z7	Putative uncharacterized protein	24.3	–	3809800	Y	0	Extracellular
D0N549	Pectinesterase	11	–	1089940	Y	0	Extracellular
D0N574	Berberine-like protein	13.6	–	1548200	Y	0	Extracellular
D0N7I7	Protein kinase	2.5	–	1292365	Y	1	Extracellular
D0NB05	Putative uncharacterized protein	9	–	1155527	Y	0	Extracellular
D0NCV1	Glucan 1,3-beta-glucosidase	22.9	–	2313600	Y	1	Extracellular
D0NG31	Putative uncharacterized protein	19.9	–	2945650	Y	0	Extracellular
D0NHK7	Putative uncharacterized protein	7	–	2852450	Y	0	Extracellular
D0NIB9	Putative uncharacterized protein	8.7	–	2831267	Y	0	Extracellular
D0NIS0	Putative uncharacterized protein	9.3	–	2802233	Y	0	Extracellular
D0NN82	Putative uncharacterized protein	2.2	–	479235	Y	0	Extracellular
D0NND3	Glycerophosphoryl diester phosphodiesterase	8.7	–	687187	Y	0	Extracellular
D0NNP2	Calcineurin-like phosphoesterase	8.9	–	533270	Y	0	Extracellular
D0NPF9	Protein kinase, putative	1.7	–	1992700	Y	2	Extracellular
D0NR36	Putative uncharacterized protein	2.7	–	2597433	Y	0	Extracellular
D0NTX2	Small cysteine-rich protein SCR91	18.7	–	3125350	Y	1	Extracellular
D0NUA5	Putative uncharacterized protein	2.4	–	16672000	Y	0	Extracellular
D0NV83	Crinkler (CRN) family protein	14.7	–	341200	N	0	Cytoplasmic
Q2M406	CRN-like CRN7	15.4	–	1099150	N	0	Cytoplasmic
D0NNH7	CRN domain-containing protein	10.8	1165250	–	N	0	Cytoplasmic
D0NQ66	Ribonuclease	2.3	1883400	–	Y	0	Extracellular
D0N6Z0	Stromal cell-derived factor 2	4.7	791820	–	Y	0	Extracellular

MIM, Mitochondrial inner membrane; SC, sequence coverage; SP, signal peptide

RXLR effector PexRD2 has been shown to interact with host MAPKKKεto suppress plant immune signaling (King *et al.*, 2014). *P. infestans* could promote PexRD2 family proteins to secrete more RxLR effectors to suppress the plant immune system. As an avirulence gene, *Avr3a* has been shown to contain the RxLR domain, which is nontoxic to potatoes containing *R3a* (Armstrong *et al.*, 2005). The RxLR effector Avr3a from *P. infestans* entered the cytoplasm of host cells to suppress the hypersensitive response of *Nicotiana benthamiana* (Bos *et al.*, 2006). The results showed that the expression of Avr3a in the mitochondrial inner membrane was upregulated 11 times under nitrogen-deficient conditions.

CRN effectors were first identified in *P. infestans* (Amaro *et al.*, 2017). They can induce plant leaf crinkling and cell death (Torto *et al.*, 2003). They have a signal peptide at N-terminus, followed by a conserved phenylalanine-leucine-alanine-lysine motif and variable C-terminal. Many previous studies have suggested that the main activity of CRN effectors is to induce plant cell death (Torto *et al.*, 2003; Haas *et al.*, 2009). CRN1 and CRN2 of *P. infestans* can cause plant cell death (Torto *et al.*, 2003).

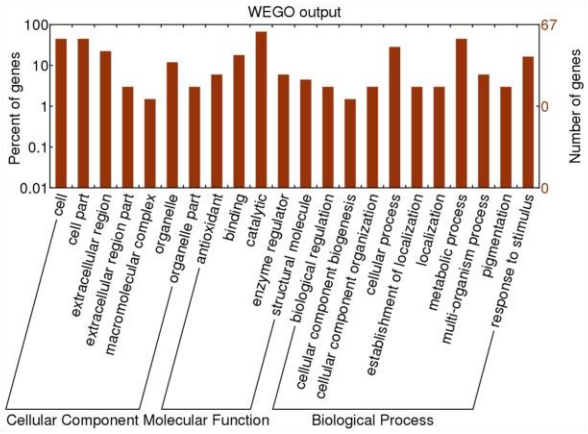

Fig. 1: Functional classification of the secretory proteins from *P. infestans*

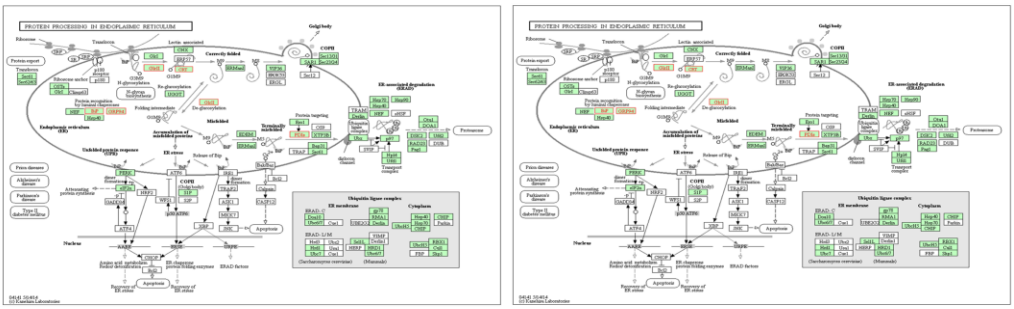

Fig. 2: Images of differentially expressed proteins in KEGG pathway from *P. infestans*. Red font: Upregulated enzymes, BiP: DOMR13, GRP94: D0N2Y9, PDIs: D0NFV4, GIcII: D0NID9, and CRT: D0NR25

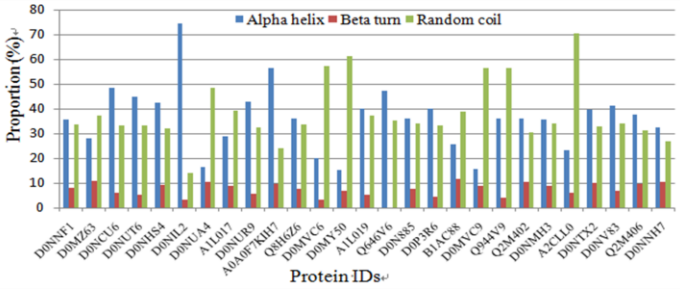

Fig. 3: Secondary structure characterization of 27 target proteins

However, recent studies have revealed that only a few CRN effectors can trigger plant cell death (Shen *et al.*, 2013; Stam *et al.*, 2013). The majority of CRN effectors can suppress the cell death triggered by PAMPs or elicitors (Shen *et al.*, 2013). A recent report has shown that CRN effectors may acquire virulence by targeting distinct sub-nuclear compartments and modifying host cell signaling (Stam *et al.*, 2013). Interestingly, most of the CRN effectors are localized in the host cell nucleus and can alter their subcellular localization to suppress cell death (Liu *et al.*, 2011; Stam *et al.*, 2013). In the present study, nine CRN effectors (including three specific proteins and six differentially expressed proteins) that did not contain a signal peptide were identified. They were all localized in the cytoplasm.

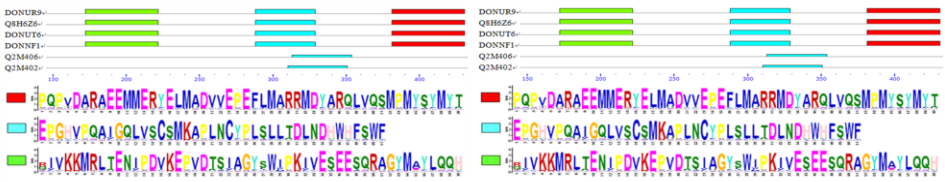

Fig. 4: Distribution of conserved motifs. Words in yellow denote letter P

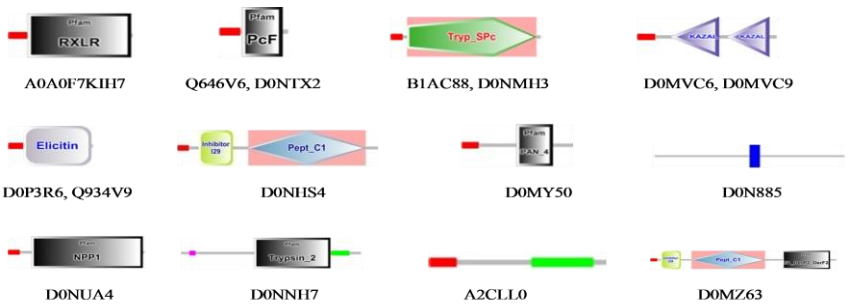

Fig. 5: Conserved domain analysis

Whether they have the pathogenicity is still not known and needs further investigation. Shen *et al.* (2013) have shown that the average expression levels of CRN effectors are much higher than those of RxLR effectors. The results also showed that the expression levels of CRN effectors were significantly higher than those of RxLR effectors.

Conclusion

This study showed that the nitrogen source influenced the expression of effectors, particularly the cytoplasmic effectors. RxLR and CRN effectors were highly expressed under nitrogen-deficient conditions. These effectors were vital in the pathogenicity of *P. infestans*, suggesting that the pathogenicity of *P. infestans* was enhanced under nitrogen-deficient conditions. The findings of the present study might be of great importance in preventing the outbreak of late blight.

Acknowledgments

This study was (give proper space throughout the paper) supported by the Key Project of Yunnan Natural Science Foundation (No. 2016FA016) and the Natural Science Foundation of China (No. 31060021).

References

Amaro, T.M., G.J. Thilliez, G.B. Motion and E. Huitema, 2017. A perspective on CRN proteins in the genomics age: evolution, classification, delivery and function revisited. *Front. Plant Sci.*, 8: 99

Armstrong, M.R., S.C. Whisson, L. Pritchard, J.I. Bos, E. Venter, A.O. Avrova, A.P. Rehmany, U. Böhme, K. Brooks, I. Cherevach, N. Hamlin, B. White, A. Fraser, A. Lord, M.A. Quail, C. Churcher, N. Hall, M. Berriman, S. Huang, S. Kamoun, J.L. Beynon and P.R. Birch, 2005. An ancestral oomycete locus contains late blight avirulence gene Avr3a, encoding a protein that is recognized in the host cytoplasm. *Proc. Natl. Acad. Sci. U.S.A.*, 102: 7766–7771

Bigelow, H. and B. Rost, 2009. Online tools for predicting integral membrane proteins. *Meth. Mol. Biol.*, 528: 3–23

Bos, J.I., T.D. Kanneganti, C. Young, C. Cakir, E. Huitema, J. Win, M.R. Armstrong, P.R. Birch and S. Kamoun, 2006. The C-terminal half of *Phytophthora infestans* RXLR effector AVR3a is sufficient to trigger R3a-mediated hypersensitivity and suppress INF1-induced cell death in *Nicotiana benthamiana*. *Plant J.*, 48: 165–176

Caillaud, M.C., S.J. Piquerez, G. Fabro, J. Steinbrenner, N. Ishaque, J. Beynon and J.D. Jones, 2012. Subcellular localization of the HpaRxLR effector repertoire identifies a tonoplast-associated protein HaRxL17 that confers enhanced plant susceptibility. *Plant J.*, 69: 252–265

Chang, L. and M. Karin, 2001. Mammalian MAP kinase signaling cascades. *Nature*, 410: 37–40

Damme, M.V., T.O. Bozkurt, C. Cakir, S. Schornack, J. Sklenar, A.M.E. Jones and S. Kamoun, 2012. The Irish potato famine pathogen *Phytophthora infestans* translocates the CRN8 kinase into host plant cells. *PLoS Pathog.*, 8:e1002875

Dong, Y., Y. Li, Z. Qi, X. Zheng and Z. Zhang, 2015. Genome plasticity in filamentous plant pathogens contributes to the emergence of novel effectors and their cellular processes in the host. *Curr. Genet.*, 62: 47–51

Donofrio, N.M., T.K. Mitchell and R.A. Dean, 2009. The significance of nitrogen regulation, source and availability on the interaction between rice and rice blast. *In*: *Advances in Genetics, Genomics and Control of Rice Blast Disease*, pp: 59–72. Wang, G.L. and B. Valent (eds.). Publishers, Springer, Dordrecht

Göhre, V. and S. Robatzek, 2008. Breaking the barriers: microbial effector molecules subvert plant immunity. *Annu. Rev. Phytopathol.*, 46: 189–215

Haas, B.J., S. Kamoun, M.C. Zody, R.H. Jiang, R.E. Handsaker, L.M. Cano, M. Grabherr, C.D. Kodira, S. Raffaele, T. Torto-Alalibo, T.O. Bozkurt, A.M. Ah-Fong, L. Alvarado and V.L. Anderson, 2009. Genome sequence and analysis of the Irish potato famine pathogen *Phytophthora infestans*. *Nature*, 461: 393–398

Hiss, J.A., J.M. Przyborski, F. Schwarte, K. Lingelbach and G. Schneider, 2008. The plasmodium export element revisited. *PLoS One*, 3: e1560

King, S.R., H. McLellan, P.C. Boevink, M.R. Armstrong, T. Bukharova, O. Sukarta, J. Win, S. Kamoun, P.R. Birch and M.J. Banfield, 2014. *Phytophthora infestans* RXLR effector PexRD2 interacts with host MAPKKK ε to suppress plant immune signaling. *Plant Cell*, 26: 1345–1359

Liu, T., W. Ye, Y. Ru, X. Yang, B. Gu, K. Tao, S. Lu, S. Dong, X. Zheng, W. Shan, Y. Wang and D. Dou, 2011. Two host cytoplasmic effectors are required for pathogenesis of *Phytophthora sojae* by suppression of host defenses. *Plant Physiol.*, 155: 490–501

Martins, I.M., F. Martins, H. Belo, M. Vaz, M. Carvalho, A. Cravador and A. Choupina, 2014. Cloning, characterization and *in vitro* and in planta expression of a glucanase inhibitor protein (GIP) of *Phytophthora cinnamomi*. *Mol. Biol. Rep.*, 41: 2453–2462

McLellan, H., P.C. Boevink, M.R. Armstrong, L. Pritchard, S. Gomez, J. Morales, S.C. Whisson, J.L. Beynon and P.R. Birch, 2013. An RxLR effector from *Phytophthora infestans* prevents re-localisation of two plant NAC transcription factors from the endoplasmic reticulum to the nucleus. *PLoS Pathog.*, 9: e1003670

Rose, J.K., K.S. Ham, A.G. Darvill and P. Albersheim, 2002. Molecular cloning and characterization of glucanase inhibitor proteins: coevolution of a counter defense mechanism by plant pathogens. *Plant Cell*, 14: 1329–1345

Sanju, S., S. Siddappa, A. Thakur, P.K. Shukla, N. Srivastava, D. Pattanayak, S. Sharma and B.P. Singh, 2015. Host-mediated gene silencing of a single effector gene from the potato pathogen *Phytophthora infestans* imparts partial resistance to late blight disease. *Funct. Integr. Genom.*, 15: 697–706

Shen, D., T. Liu, W. Ye, L. Liu, P. Liu, Y. Wu, Y. Wang and D. Dou, 2013. Gene duplication and fragment recombination drive functional diversification of a superfamily of cytoplasmic effectors in *Phytophthora sojae*. *PLoS One*, 8: e70036

Snoeijers, S., A. Pérez-García, M.H.A.J. Joosten and P.J.G.M. De Wit, 2000. The effect of nitrogen on disease development and gene expression inbacterial and fungal plant pathogens. *Eur. J. Plant Pathol.*, 106: 493–506

Stam, R., J. Jupe, A.J. Howden, J.A. Morris, P.C. Boevink, P.E. Hedley and E. Huitema, 2013. Identification and characterisation CRN effectors in *phytophthora capsici* shows modularity and functional diversity. *PLoS One*, 8: e59517

Tian, M. and S. Kamoun, 2005. A two disulfide bridge Kazal domain from *Phytophthora* exhibits stable inhibitory activity against serineproteases of the subtilisin family. *BMC Biochem.*, 6: 15

Tian, M., J. Win, J. Song, R.V.D. Hoorn, E.V.D. Knaap and S. Kamoun, 2007. A *Phytophthora infestans* cystatin-like protein targets a novel tomato papain-like apoplastic protease. *Plant Physiol.*, 143: 364–377

Torto, T.A., S. Li, A. Styer, E. Huitema, A. Testa, N.A. Gow, P.V. West and S. Kamoun, 2003. EST mining and functional expression assays identify extracellular effector proteins from the plant pathogen *Phytophthora*. *Genom. Res.*, 13: 1675–1685

Vetukuri, R.R., S.C. Whisson and L.J. Grenville-Briggs, 2017. *Phytophthora infestans* effector Pi14054 is a novel candidate suppressor of host silencing mechanisms. *Eur. J. Plant Pathol.*, 149: 771–777

Wang, Y., J. Wu, Z.Y. Park, S.G. Kim, R. Rakwal, G.K. Agrawal, S.T. Kim and K.Y. Kang, 2011. Comparative secretome investigation of *Magnaporthe oryzae* proteins responsive to nitrogen starvation. *J. Proteom. Res.*, 10: 3136–3148

Zhou, X.G., P. Yu, C. Dong, C.X. Yao, Y.M. Ding, N. Tao and Z.W. Zhao, 2016. Proteomic analysis of mycelial proteins from *Magnaporthe oryzae* under nitrogen starvation. *Genet. Mol. Res.*, 15: *Genet. Mol. Res.*, 15: 1-10

(Received 14 May 2018; Accepted 26 May 2019)